Nanomed. J. 7(1): 1-12, Winter 2020

REVIEW PAPER

Bimodal magnetic resonance imaging-computed tomography nanoprobes: A Review

Fatemeh Bakhtiari-Asl [1, 2], Baharak Divband [3, 4], Asghar Mesbahi [1, 2], Nahideh Gharehaghaji [5*]

[1]Medical Radiation Sciences Research Group, Tabriz University of Medical Sciences, Tabriz, Iran
[2]Department of Medical Physics, Faculty of Medicine, Tabriz University of Medical Sciences, Tabriz, Iran
[3]Dental and Periodontal Research Center, Tabriz University of Medical Sciences, Tabriz, Iran
[4]Department of Inorganic Chemistry, Faculty of Chemistry, University of Tabriz, C.P. 51664, Tabriz, Iran
[5]Department of Radiology, Faculty of Paramedicine, Tabriz University of Medical Sciences, Tabriz, Iran

ABSTRACT

Bimodal imaging combines two imaging modalities in order to benefit from their advantages and compensate the limitations of each modality. This technique could accurately detect diseases for diagnostic purposes. Nanoparticles simultaneously offer diagnostic data via various imaging modalities owing to their unique properties. Moreover, bimodal nanoprobes could be incorporated into theranostic systems for the design of multifunctional agents. Magnetic resonance imaging (MRI) and computed tomography (CT) are frequently used as noninvasive imaging modalities. These powerful, noninvasive diagnostic techniques used for the imaging of soft and hard tissues, respectively. However, MRI has low sensitivity and is not suitable for the imaging of bony structures. On the other hand, low soft tissue contrast is a major limitation of CT. Therefore, the development of various contrast agents that are proper for bimodal MRI/CT nanoprobes could largely influence modern medicine. This review aimed to specifically focus on the imaging properties of bimodal MRI/CT nanoprobes and their biomedical applications.

Keywords: *Bimodal Imaging, Biomedical Applications, CT, MRI, Nanoprobe*

How to cite this article
Bakhtiari-Asl1 F, Divband B, Mesbahi A, Gharehaghaji N. Bimodal magnetic resonance imaging-computed tomography nanoprobes: A Review. Nanomed J. 2020; 7(1): 1-12. DOI: 10.22038/nmj.2020.07.01

INTRODUCTION

Today, bimodal imaging has attracted great attention for biomedical applications. To date, numerous biomedical imaging modalities have been applied for the detection of diseases, including magnetic resonance imaging (MRI), computed tomography (CT), positron emission tomography (PET), single-photon emission computed tomography (SPECT), ultrasonography, and optical imaging [1]. Each imaging modality provides particular diagnostic data and has specific advantages and limitations [2]. The differences in these modalities are based on several factors, such as their image formation [3], resolution, sensitivity [4], and provision of anatomical/structural or functional/metabolic data [5].

In CT, SPECT and PET, ionizing radiation is used for image formation, while MRI and ultrasonography require the use of non-ionizing radiation [6]. MRI is mainly used for the imaging of soft tissues with high resolution; however, this technique has low sensitivity [7], while PET provides images with high sensitivity and poor spatial resolution [8]. Some biomedical imaging tools (e.g., CT) are mainly used to provide important structural and anatomical data [7]. On the other hand, modalities such as SPECT and PET are used for the preparation of functional/metabolic data on the examined tissues [9].

In bimodal imaging, the limitations of each modality could be compensated with the advantages of another modality. Therefore, bimodal imaging plays a key role in the accurate diagnosis of various diseases.

Advancement in nanotechnology has resulted in the development of new nanomaterials as potential imaging contrast agents. Nanomaterial-based contrast agents have several physical and chemical advantages, including the tunability of the surface, size, and shape of nanoparticles [10] and conjugation with biological molecules

* *Corresponding Author Email: gharehaghajin@tbzmed.ac.ir*
Note. This manuscript was submitted on September 3, 2019; approved on November 1, 2019

to identify the target of interest [11]. In addition, nanomaterial combinations could be applied in the structure of bimodal and multimodal imaging probes [12]. To date, various nanoprobes have been introduced for bimodal imaging techniques, including PET/CT [13], ultrasound/CT [14], ultrasound/MRI [15], PET/MRI [16], MRI/SPECT [17], MR/optical imaging [18], SPECT/fluorescence imaging [19], MRI/CT [20], SPECT/CT [21], and fluorescent /CT [22].

Basics

Among various medical imaging modalities, MRI and CT are most commonly used for diagnostic purposes. MRI is a powerful, noninvasive diagnostic technique, which provides anatomical data from the internal organs of the body. Furthermore, MRI provides sectional images of soft tissues with high spatial resolution by applying non-ionizing radiofrequency pulses. MRI could also provide physiological and even molecular data although the latter is limited due to its poor sensitivity [23]. Inherent contrast in MRI depends on the differences in the T1 and T2 relaxation times of the tissues and their proton density [24]. If there are slight differences between the relaxation times of normal tissues and lesions, the inherent contrast of MRI is inadequate, which in turn leads to low sensitivity. MRI contrast agents overcome this limitation by affecting the relaxation processes.

MRI contrast agents are classified into two categories. The first category is T1 agents, which are mainly based on gadolinium and manganese ions that mostly reduce the T1 relaxation time of water protons and make brightness in the accumulation region. The second category of MRI contrast agents are T2 agents (e.g., superparamagnetic iron oxide nanoparticles), which significantly reduce the T2 relaxation time of water protons, providing the dark region on the image. The ability of an MRI contrast agent to change relaxation rates is referred to as relaxivity (r). Higher relaxivity is associated with better contrast enhancement. Based on the changes in T1 and T2 relaxation rates, relaxivities are classified as r1 and r2, respectively. Although proton (^{1}H)-based MRI is able to provide excellent images of soft tissues, it is not considered suitable for the imaging of bony tissue, which is another limitation of MRI [25, 26]. CT has extensive clinical application as a noninvasive imaging modality that provides anatomical data based on the difference in the X-ray absorption of various tissues. Some of the key advantages of CT include high resolution, three-dimensional tomographic imaging, cost-efficiency, short acquisition time, availability, and development of hybrid imaging systems (e.g., PET/CT and SPECT/CT). Due to their high X-ray absorption, hard tissues (e.g., bony structures) are viewed with high contrast in CT images, while this modality has low soft tissue contrast [27]. Therefore, CT contrast agents consisting of materials with a high atomic number and high X-ray attenuation coefficients are used to improve the soft tissue contrast of this method [28]. In addition, the combination of CT and MRI in bimodal imaging leads to overcome the low soft-tissue contrast in CT [23, 29].

Currently, conventional CT contrast agents are mainly based on barium sulfate suspensions and iodinated compounds. Barium ions are toxic, and barium (Z=56, K-edge energy=37.4 keV) is clinically used as barium sulfate only for the imaging of the gastrointestinal tract [30]. With respect to nanomaterials, Liu et al. have reported $BaYbF_5$@SiO_2@PEG nanoparticles as CT contrast agent [31]. Moreover, iodine molecules with a high atomic number (Z=53, K-edge energy=33.2 keV) could effectively absorb X-ray photons. However, small iodine molecules are rapidly eliminated by the kidneys and have a short blood circulation time [32]. Recently, nanomaterials such as bismuth and gold nanoparticles have attracted great attention to be used as CT contrast agents due to their high contrast enhancement, long circulation time, and low toxicity. Bismuth (Z=83, K-edge energy=90.5 keV) has higher X-ray attenuation and lower toxicity compared to iodine [33]. Various bismuth-based nanoparticles have been investigated as CT contrast agents, such as Bi_2S_3 nanodots [34], Bi_2Se_3 [35], and Bi_2O_3 nanoparticles [27]. Gold has a high atomic number (Z=79) and K-edge energy of 80.7 keV and provides stronger X-ray attenuation compared to iodine and barium sulfate, especially at the energy levels that are used clinically [36]. Furthermore, gold nanoparticles exhibit unique properties, such as high compatibility, facile surface modification, and passive tumor targeting [37, 38]. To date, various nanomaterials have been assessed as bimodal MRI/CT nanoprobes. This review aimed to summarize the findings regarding bimodal MRI/CT nanoprobes, as well as their properties and applications, for diagnostic purposes.

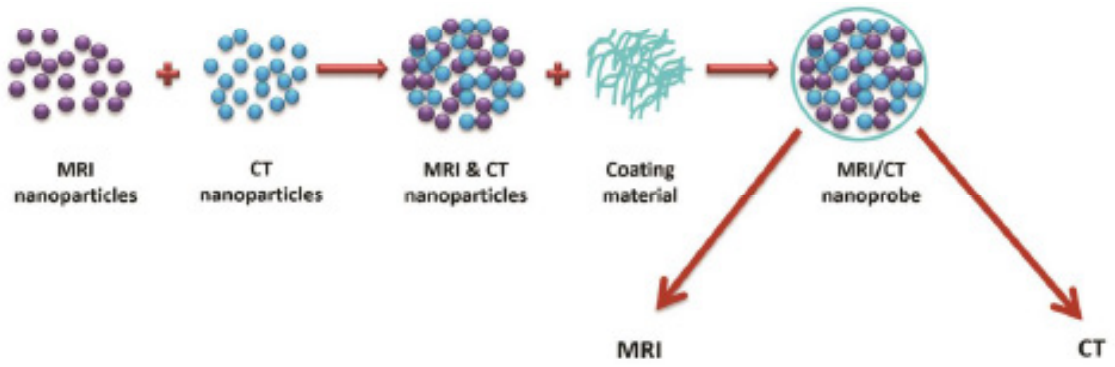

Fig 1. Schematic View of a Bimodal MRI/CT Nanoprobe

Bimodal MRI/CT nanoprobes

Nanoprobes with high relaxivity (r1 for T1 contrast agents and r2 for T2 agents) and high X-ray attenuation are proper candidates for bimodal MR/CT imaging. Fig 1 depicts the schematic view of a bimodal nanoprobe for MRI/CT.

In general, the difference in the relaxivity of nanoparticles depends on several factors, such as the applied magnetic field strength, nanoparticle size, type and thickness of the surface coating material, magnetic moment, aggregation of the particles, and number of the water protons that are available to magnetic ions [39]. The increasing of field strength leads to the reduction of r1 relaxivity, while the increasing of r2 to its maximum value and then its decreasing at higher field strengths is occurred. Furthermore, the reduction of r1 and increasing of r2 is resulted from increased aggregate size [40].

Smaller nanostructures have higher surface-to-volume ratio, which causes access of many gadolinium ions to water protons, leading to higher r1 relaxivity [41]. In case of iron oxide nanoparticles, the increasing of the mean diameter of the particles leads to higher r2 relaxivity. On the other hand, particles with smaller sizes have low r2/r1 and are appropriate candidates as T1 contrast agents. Larger iron oxide nanoparticles have shorter blood half-life. Blood kinetics is also strongly affected by the ionic characteristics of coating materials [42]. Larger ligand size decreases the access of nanostructures to water protons, thereby leading to smaller r1 and r2 relaxivity values [43]. The studies regarding the effects of coating materials and their thickness on r2 relaxivity have proposed different results [44].

In general, materials with high atomic numbers offer higher X-ray attenuation, and X-ray energy is considered to be a key influential factor in its attenuation. When the X-ray energy is equal to or partially larger than the K-edge energy of an atom, X-ray attenuation is higher [45]. To date, various *in-vitro* and *in-vivo* studies have been conducted using various materials in order to investigate their biocompatibility and potential as MRI/CT nanoprobes. These agents have been discussed extensively in the following sections.

Gadolinium-based MRI/CT nanoprobes

Gadolinium (Gd) is the most commonly used MRI contrast agent. Paramagnetic gadolinium has seven unpaired 4f electrons and produces a large magnetic moment, which make this material an excellent relaxation-enhancing agent. However, free gadolinium ions are toxic and maintained in various body tissues, such as the liver, spleen, and bones. Chelation of gadolinium by ligands leads to the reduction of its toxicity. Despite the clinical utility of gadolinium chelates, they do not have high sensitivity and their renal clearance is fast. On the other hand, gadolinium nanoparticles are potential candidates to be used as MRI contrast agents.

The concentration of gadolinium ions in nanoparticles could decrease the toxicity of the ions, and enhance the MRI T1 contrast [46]. In addition, gadolinium oxide (Gd_2O_3) nanoparticles have a large surface-to-volume ratio and higher relaxivity compared to gadolinium chelates [47]. Therefore, these materials have been frequently

studied as MRI contrast agents [43, 48-51]. It is also notable the high atomic number of gadolinium provides high contrast in CT imaging [52-54].

Gadolinium/gold nanoprobes

Gadolinium and gold nanostructures have been frequently studied as MRI/CT bimodal nanoprobes. Gold nanoparticles have important properties, which are effective in CT contrast enhancement. Some of these properties include high atomic number and X-ray absorption coefficient. In addition, the tunable size and shape of gold nanoparticles allow their surface modification with various functional groups. Gold nanoparticles are also nontoxic and have high biocompatibility [31, 38, 55].

In the study by Tian et al., polyacrylic acid was used as the bridge between the gadolinium metal organic framework (MOF) and gold nanoparticles in the hybrid GdMOF-PAA-Au nanocomposite so as to provide stronger interaction between gadolinium MOF and gold nanoparticles. Moreover, the nanocomposite exhibited the r1 of 4.9 $mM^{-1}s^{-1}$ at 4.7 T, which was slightly higher than Magnevist as a gadolinium chelate at the same field strength. The nanocomposite also demonstrated enhanced CT contrast even at low concentrations of gold (1.66 mg/ml) [56].

Gadolinium-functionalized gold nanorods have also been investigated as bimodal MRI/CT contrast agents. In this nanoprobe, amphiphilic gadolinium chelates are connected via a non-covalent bond to the outer surface of gold nanorods, thereby providing high r1 relaxivity (21.3 $mM^{-1}s^{-1}$ gadolinium per ion at 9.4 T) due to the direct access of gadolinium ions to water protons. Furthermore, the high surface-to-volume ratio of gold nanorods provides the opportunity for the binding of more gadolinium ions to the surface of the nanorods. Additionally, the large surface of the nanorods also improved the X-ray attenuation of CT images, so that the nanoprobe could enhance contrast at low gold concentrations (e.g., 1.31 mg ml^{-1}) [57].

In another study in this regard, the gadolinium chelate coated with gold nanoparticles (Au@DTDTPA-Gd) were evaluated in *in-vitro* and *in-vivo* CT and MRI. In the mentioned research, CT imaging was performed using synchrotron radiation computed tomography (SRCT), which provided monochromatic X-ray beams with five-fold intensity compared to the X-rays emitted from conventional sources. Furthermore, SRCT could provide the quantification of the contrast agent concentration in tissues. In the mentioned study, MRI was performed using a 7.0 T instrument, and nanoparticles were detected in both CT and MRI modalities even at low concentrations of gold (10 mg/ml^{-1}) and gadolinium (5 mM). In addition, gadolinium was reported to slightly contribute to the SRCT image contrast. *In-vivo* animal study indicated the circulation of nanoparticles in blood without unsuitable accumulation in the liver, lungs, and spleen [58].

In another research, Zhou et al. synthesized PEGylated gadolinium-loaded polyethylenimine-entrapped gold nanoparticles (Gd@Au PENPs) and examined the nanoprobe for *in-vitro* and *in-vivo* MR/CT imaging. According to the findings, the r1 (17.8 $mM^{-1}s^{-1}$ at 3.0 T) and CT values of the Gd@Au PENPs were higher than Magnevist and Omnipaque, respectively. On the same note, an *in-vivo* study was conducted on mice, demonstrating that the CT values of the inferior vena cava and liver increased on the post-contrast images, while slight contrast enhancement was observed in the kidney region. On the other hand, the increasing of the administrated dose led to the enhancement of various blood vessels, including the aorta, inferior vena cava, portal vein, and renal vein. The T1-weighted MR images also clearly revealed the inferior vena cava and aorta after the injection of the Gd@Au PENPs. No significant histological changes were reported 30 days after the injection of the nanoparticles, which confirmed the biocompatibility of the nanoparticles at the applied dosage [59]. Bovine serum albumin-coated gold nanoparticles (Au@BSA) containing Gd(III) were assessed in another study with the aim of providing CT and T1-weighted MRI contrast. According to the findings, the contribution of the Gd(III) ions and gold nanoparticles led to the higher X-ray attenuation of the contrast agent. Additionally, higher r1 than Magnevist (5.04 and 3.54 $mM^{-1}s^{-1}$, respectively) was obtained at 3.0 T [60]. According to a research conducted by Li et al., multifunctional Gd(III)-loaded dendrimer-based gold nanoparticles (Gd-Au DENPs) were used in the bimodal MR/CT imaging of breast cancer cells *in-vitro* and *in-vivo*. The MR and CT imaging of human MCF-7 cancer cells and xenograft tumor model showed enhanced images [61]. In addition, the RGD-peptide-modified multifunctional dendrimer-entrapped gold nanoparticles that were loaded

with gadolinium chelator/Gd(III) complexes (Gd-Au DENPs-RGD) were assessed for the targeted imaging of αvβ3 integrin-overexpressing cancer via dual mode CT/MRI. According to the findings, the Gd-Au DENPs-RGD nanoprobe was nontoxic and offered X-ray attenuation, and the r1 value of 2.643 $mM^{-1}s^{-1}$ at 3.0 T [62].

In the study by Li et al., gadolinium and gold atoms were simultaneously loaded into the zwitterionic glutathione (GSH) shell with cyclic Asn-Gly-Arg (cNGR) peptide modification, and the capability of ultra-small cNGR-Au:Gd@GSH nanomolecules for *in-vitro* and *in-vivo* bimodal MRI/CT was investigated. The r1 relaxivity of 38.4095 $mM^{-1}s^{-1}$ at 3.0 T, which was 8.6 times higher than Magnevist (4.46 $mM^{-1}s^{-1}$), confirmed the high potential of nanomolecules for MRI. Moreover, the CT attenuation enhancements of the nanomolecules were approximately 18, 25, 66, 93, 136, and 180 times higher compared to iohexol in the abdomen, chest, head, maxillofacial region, centrum, and lower-limb sequences, respectively.

The *in-vivo* results of MRI and CT in mice have also demonstrated the great potential of cNGR-Au:Gd@GSH nanomolecules for the bimodal MRI/CT of tumor angiogenesis [63].

Gadolinium/silver nanoprobes

Although silver iodide colloid has been applied as a CT contrast agent in animal models, its usage in human subjects has been precluded due to its high toxicity [64]. However, *in-vitro* biocompatibility studies have indicated that the substitution of silver in hydroxyapatite crystals could resolve the toxicity issue [65]. In a study by Madhumathi et al., silver (Ag) and gadolinium ions co-substituted hydroxyapatite nanoparticles were synthesized with various atomic ratios of silver and gadolinium (Ag:Gd=0.25:0.25, 0.25:0.5, and 0.25:0.75) for dual mode CT/MRI. Afterwards, they were compared with the nanoparticles substituted with only silver or gadolinium ions. According to the obtained results, the samples of Ag^{+} and Gd^{3+} ions that co-substituted hydroxyapatite nanoparticles had higher contrast, so that the optimal bimodal contrast was achieved using the Ag:Gd ratio of 0.25:0.75. In the mentioned study, X-ray attenuation was affected by both the silver and gadolinium ions, and the nanoparticles with the highest gadolinium content provided the highest MRI contrast as well [66].

Gadolinium/Iodine nanoprobes

Iodine has a high atomic number, and iodine compounds have been widely used as clinical CT contrast agents. In a study in this regard, Ahmad et al. investigated the potential of various iodine compounds coated Gd_2O_3 nanoparticles for bimodal CT and T1 MRI. According to the findings, the samples had higher X-ray attenuation and longitudinal relaxivity (r1=26-38 $mM^{-1}s^{-1}$) compared to conventional contrast media with 1.5 T field strength. The cell viability test indicated that the samples were biocompatible. Contrast enhancement was also observed in both CT and MRI after the injection of the nanoparticles to mice, which confirmed the dual imaging potential of Gd_2O_3 nanoparticles coated with iodine compounds. On the other hand, the magnetic properties of gadolinium and its high amount per Gd_2O_3 nanoparticles, as well as the high atomic number of gadolinium resulted in the capability of the iodine compounds coated Gd_2O_3 nanoparticles in bimodal MR/CT imaging without the need for additional functionalization [52].

Other gadolinium-based MRI/CT nanoprobes

Polyacrylic acid (PAA)-capped GdF_3 nanoplates have been reported to have the high r1 value of 15.8 L/mmol at 0.5 T (four times higher than Gd-DTPA). This has been attributed to the two-dimensional structure of the nanoplates, which enables the provision of a large surface area to volume compared to the nanoplates with spherical nanostructures. In this regard, the X-ray attenuation of nanoplates has been reported to be higher compared to iohexol (a commercial CT contrast agents) at similar concentrations [20]. In another research, a PEGylated Dy-doped $NaGdF_4$ nanoprobe was prepared to be used as a T1/T2-weighted MRI/CT imaging probe. The r1 and r2 relaxivity of the nanoprobe at 9.4 T was reported to be 5.17 and 10.64 $mM^{-1}s^{-1}$, respectively. Moreover, this nanoprobe showed high X-ray attenuation (44.70 HU L/g). *In-vivo* findings exhibited its efficient contrast enhancement in the kidneys, spleen, and liver of mice 24 hours after injection [67].

In a research conducted by Wang et al., PEGylated $BaGdF_5$ (PEG-$BaGdF_5$) nanoparticles showed positive MRI contrast and proper X-ray attenuation *in-vitro*. In the mentioned study, the connection of the RGD peptide to the nanoparticles surface (RGD-PEG-$BaGdF_5$) was

performed for tumor vasculature targeting. The RGD-PEG-$BaGdF_5$ or PEG-$BaGdF_5$ nanoparticles were intravenously injected to VX2 tumor-bearing mice, and MR/CT imaging was carried out. The obtained results were indicative of higher MRI signal enhancement and CT value in the tumor site in the RGD-PEG-$BaGdF_5$ group. Furthermore, it was suggested that RGD-PEG-$BaGdF_5$ could be used in bimodal MRI/CT for the detection of various solid tumors [68].

In another study, AR-Bi@SiO2-Gd/DOX nanoparticles were introduced for accurate tumor detection and targeting. The surface of the nanoparticles was composed of AREYGTRFSLIGGYR (AR), which is an MCF-7 breast tumor-homing peptide. According to the findings, the applied nanoparticles could significantly increase MRI and CT imaging contrast, while inhibiting tumor growth as well [69].

Table 1 summarizes the MRI and CT properties of various gadolinium-based MRI/CT nanoprobes.

Manganese-based MRI/CT nanoprobes

Manganese (Mn) is another paramagnetic ion used as an MRI contrast agent. Since free manganese is toxic, its chelating or coating in the nanoparticle form may prevent the premature loss of free manganese. The only FDA approved manganese-chelate, manganese-DPDP or mangafodipir trisodium (Teslascan) is an organ-specific agent used for liver imaging. Recently, manganese oxide particles (e.g., MnO, MnO_2, and Mn_3O_4) have been designed as MRI contrast agents [70]. It has also been suggested that manganese-based nanoparticles have the potential for dual mode MRI/CT. Manganese-chelated dendrimer-entrapped gold nanoparticles modified with hyaluronic acid {(Au0)100G5.NH2-FI-DOTA(Mn)-HA} nanoparticles were reported as a bimodal probe for the targeted CT and MRI of hepatocellular carcinoma (HCC). The r1 relaxivity of these nanoparticles was calculated to be 5.42 $mM^{-1}s^{-1}$ (0.5 T field strength).

Table 1. Gadolinium Based MRI/CT Nanoprobes

Gd based MRI/CT nanoprobes	Nanoprobe	MRI field intensity (T)	r1 relaxivity ($mM^{-1}s^{-1}$)	CT	Reference
Gd/Au nanoprobes	GdMOF-PAA-Au	4.7	4.9	Enhanced CT contrast at Au concentrations as low as 1.66 mg/ml	56
	Gd functionalized gold nanorods	9.4	21.3 per Gd ion	Enhanced contrast at Au concentration as low as 1.31 mg/ml	57
	Au@DTDTPA-Gd	7.0	-	Enhanced CT contrast at the low content of Au (10 mg ml-1)	58
	Gd@Au PENPs	3.0	17.8	Increasing of CT value of inferior vena cava, liver and different blood vessels	59
	Au@BSA-Gd-DTPA	3.0	5.04	high X-ray attenuation due to contribution of Gd (III) ions and gold	60
	Gd-Au DENPs	3.0	-	Enhanced CT images of human MCF-7 cancer cells and xenograft tumor model	61
	Gd–Au DENPs-RGD	3.0	2.643	X-ray attenuation for targeted imaging of αvβ3 integrin-overexpressing cancer	62
	cNGR-Au:Gd@GSH	3.0	38.4095	CT attenuation enhancements about 18-180 times higher than Iohexol	63
Gd/Ag nanoprobe	Ag and Gd ions co-substituted hydroxyapatite	1.5	-	Best contrast using the percentage of Ag:Gd = 0.25:0.75	66
Gd/I nanoprobes	Various iodine compounds coated Gd_2O_3 nanoparticles	1.5	26-38	Combination of high atomic number of Gd and the iodine compounds in CT contrast	52
Other Gd based nanoprobes	Polyacrylic acid (PAA)-capped GdF_3 nanoplates	0.5	15.8 L/(mmol s)	X-ray attenuation higher than the commercial CT contrast agent, Iohexol	20
	PEGylated Dy-doped $NaGdF_4$	9.4	5.17	High X-ray attenuation (44.70 HU L/g)	67

Table 1. Gadolinium Based MRI/CT Nanoprobes In addition, the CT contrast was reported to linearly increase at higher gold concentrations. Contrast enhancement was also observed in the post-contrast MRI and CT images of HCC cells *in-vitro* and orthotopically transplanted HCC tumors *in-vivo* [71].

In a research in this regard, image contrast enhancement in CT and 1.0 T MRI using Au NPs@ PEG-Mn^{2+} exhibited the great potential of the nanoparticles to use as bimodal imaging probe. Furthermore, the *in-vivo* studies conducted on mice models indicated long blood retention (minimum of 90 minutes), which minimizes the repeated injection of the contrast agent [72].

Iron Oxide- and Iron-based MRI/CT nanoprobes

Superparamagnetic iron oxide nanoparticles are considered to be the most appropriate T2 contrast agents due to their safety and efficacy [73, 74]. Iron oxide is commonly used as an MRI contrast agent in the form of Fe_3O_4 (magnetite) and maghemite (γ-Fe_2O_3). However, maghemite has been reported to have higher stability compared to magnetite. Both these compounds have advantages such as biocompatibility, chemical stability, and high magnetic moment. To date, various iron oxide- and iron-based nanoprobes have been introduced as potential contrast agents for bimodal MRI/CT with wide biomedical applications. The studies in this regard have been reviewed in the following sections.

Iron oxide-based MRI/CT nanoprobes

Most of studies regarding iron oxide-based MRI/CT nanoprobes have been focused on gold nanoparticles as the CT contrast enhancement material. Iron oxide/gold nanoprobes with various coatings and functionalizing materials have been synthesized with various methods and sizes, showing variable relaxivities and X-ray attenuation. The biocompatibility of these nanoprobes has also been investigated, and they have been applied for biomedical imaging purposes.

In a study in this regard, Kim et al. reported the strong X-ray attenuation of PEG-coated gold@ iron oxide core shell nanoparticles, which was higher compared to iodine contrast agents at the same concentration. The high intensity of the CT image resulted from the presence of gold in the nanoprobe structure. In addition, the darkness of MRI images acquired with 1.5 T field was increased with increasing of the concentration. The MRI signal intensity produced by the nanoparticles was reported to be mild. The MTT results indicated that the nanoparticles caused no significant toxicity in cells even at high concentrations (e.g., 1 mg/ml) [75].

In another study, a green synthesis approach was applied for the preparation of Fe_3O_4/Au hybrid nanoparticles. The nanoparticles provided the high r2 value of 124.2 $mM^{-1}s^{-1}$ at 1.5 T, and their CT contrast was also higher compared to iodine contrast agents. Therefore, the nanoparticles were considered appropriate for stem cell imaging [76]. The Fe_3O_4@Au nanocomposite that was prepared using the controlled co-precipitation method had the relatively high r2 value of 71.55 $mM^{-1}s^{-1}$ (3.0 T), while exhibiting high X-ray attenuation properties. In this regard, the *in-vitro* imaging of cancer cells, *in-vivo* CT imaging of subcutaneous tissue, and MRI of liver suggested that the nanoparticles had the potential to be used as bimodal imaging nanoprobe [77].

In another research, Fe_3O_4@Au-mPEG-PEI. NHAc nanoparticles had the r2 value of 146.07 $mM^{-1}s^{-1}$ (3.0 T), and the X-ray attenuation of the nanoparticles was higher compared to Omnipaque at the same concentrations of gold or iodine. Clearly detected mouse liver in the MRI images and rabbit aorta and liver in CT images confirmed the great potential of these nanoparticles for use as CT/MRI bimodal imaging probe. Moreover, the nanoparticles could be developed as targeted bimodal MRI/CT probes for the detection of cancer in the early stages due to the presence of numerous amines on the surface of PEI and possibility of further modification by various targeting ligands [78].

An evaluation of water-soluble Au-Fe_3O_4 heterostructured nanoparticles indicated that the signal intensity of the nanocomposite in MRI images decreased at higher iron concentrations. The r2 value at 1.5 T was estimated 136.4 $mM^{-1}s^{-1}$, which was close to commercial contrast agents. In addition, the CT signal intensity was reported to continuously increase with the increment in concentration. For *in-vivo* imaging, the nanoparticles were injected to rabbits, and the right ventricle and liver could be clearly detected in CT and MRI, respectively, confirming the great potential of the nanoparticles for bimodal imaging [79]. In another study in this regard, the gold nanocage functionalized with ultra-small

Fe_3O_4 nanoparticles (F-AuNC@Fe_3O_4) provided the targeted CT and T1/T2 MRI of tumor bearing nude mice. Furthermore, the ultra-small size of the Fe_3O_4 nanoparticles and their relaxivity values (r1=6.263 $mM^{-1}s^{-1}$ and r2=28.117 $mM^{-1}s^{-1}$) at 1.41 T resulted in the high signal enhancement of T1- and T2-weighted MRI. On the other hand, the gold nanocages provided strong X-ray attenuation. In this regard, the results of *in-vivo* studies indicated that F-AuNC@Fe_3O_4 had a long circulation time, which was associated with its accumulation in the tumor and rapid elimination through renal clearance [80].

The potential of Fe_3O_4/TaO_x core-shell nanoparticles as bimodal MRI/CT nanoprobe for accurate cancer diagnosis was confirmed in the study by Li et al. In the mentioned research, the r2 value was calculated to be 81.156 $mM^{-1}s^{-1}$ at 3.0 T. In addition, the continuously increase of signal enhancement was denoted in CT images without saturation. An *in-vivo* study in tumor bearing rats demonstrated the clear imaging of newly formed tumor blood vessels in CT, while MRI images were used for the evaluation of the tumor microenvironment [81].

In a research in this regard, Zhu et al. used a new method for the synthesis of a PEGylated iron oxide@bismuth sulfide (PEG-ION@Bi_2S_3) core-shell nanocomposite for MRI and CT bimodal imaging. According to the findings, the r2 of the water soluble nanocomposite (130.4 $mM^{-1}s^{-1}$ at 3.0 T) was close to that of commercial MRI contrast agents. On the other hand, the CT contrast of the nanocomposite, which was provided by the Bi_2S_3 nanoshell, was reported to be higher compared to iobitridol as a commercial CT contrast agent [82].

In another study, Badrigilan et al. developed superparamagnetic iron oxide/bismuth oxide (GQDs-Fe/Bi) nanoparticles coated with graphene quantum dots (GQDs) as a multifunctional nanohybrid for bimodal MRI/CT and photothermal therapy.

According to the obtained results, the theranostic nanoprobe had proper efficacy in CT with higher X-ray enhancement (44.4 $HUmM^{-1}$) compared to urografin as a conventional CT contrast agent. In addition, the ability of the nanohybrid for T2 shorting at 1.5 T MRI was confirmed with the r2 relaxivity of 62.34 $mM^{-1}s^{-1}$ [83]. The MRI and CT properties of various iron oxide-based MRI/CT nanoprobes are presented in Table 2.

Table 2. Iron Oxide Based MRI/CT Nanoprobes

Iron oxide (IO) based nanoprobes	Nanoprobe	MRI field intensity (T)	r2 relaxivity ($mM^{-1}s^{-1}$)	CT	Reference
IO/AU nanoprobes	PEG coated gold@iron oxide	1.5	-	X-ray attenuation higher than iodine contrast agent	75
	Fe_3O_4/Au hybrid	1.5	124.2	CT contrast higher than iodine contrast agents	76
	Fe_3O_4@Au	3.0	71.55	In vivo CT of subcutaneous tissue	77
	Fe_3O_4@Au-mPEG-PEI.NHAc	3.0	146.07	X-ray attenuation higher than Omnipaque, CT of rabbit aorta and liver	78
	Au–Fe_3O_4	1.5	136.4	CT of the right ventricle and liver in rabbits	79
	F-AuNC@Fe_3O_4	1.41	28.117	Strong X-ray attenuation by Au nanocages, Long circulation time, accumulation in the tumor and rapid elimination by renal clearance	80
IO/Bi nanoparticles	PEG-ION@Bi_2S_3	3.0	130.4	CT contrast higher than iobitridol as commercial CT contrast agent	82
	GQDs-Fe/Bi	1.5	62.34	Higher X-ray enhancement (44.4 HU.mM−1) than Urografin as conventional CT contrast agent	83
Other IO based nanoprobe	Fe_3O_4/TaO_x	3.0	81.156	Clearly imaging of newly formed tumor blood vessels in rat	81

Nano zeolites and porous inorganic materials have been used as carriers for Fe_3O_4 nanoparticles, and the resultant nanocomposite has shown considerably high r2 values [73, 84, 85]. In addition, zeolite has been used in other bimodal imaging methods.

Iron-based MRI/CT nanoprobes

FePt nanoparticles were synthesized using the polyol method with the diameters of three, six, and 12 nanometers. In *in-vitro* T2- and T2*-weighted imaging, all the samples were reported to show inverse MRI image contrast. Among various sizes of the nanoparticles, 12-nanometer FePt was reported to provide the highest negative contrast. Furthermore, the *in-vitro* CT results demonstrated that the positive contrast effects of the 12-nanometer FePt was equal to commercial iodine contrast agent, and the contrast effects of three- and six-nanometer FePt was observed to be twice higher than the iodine contrast agent at the same concentration. The high X-ray attenuation of the nanoparticles was attributed to the Pt component. On the other hand, the biodistribution assessment of the samples in mice revealed that all the three sizes of the nanoparticles could be cleared from major body organs after one week. The highest serum concentration and circulation half-life were also reported with the use of the 12-nanometer FePt, while the highest brain concentration was observed with the use of the three-nanometer FePt, making it an ideal subject for the future investigation of multimodal brain imaging. In addition, the highest MRI and CT contrast was obtained with the use of the 12-nanometer FePt. A monoclonal antibody conjugated with FePt nanoparticles was also used for the targeting of the Her2/neu expression in the cancer lesions in mice, and the obtained results confirmed the capability of the nanoparticles in bimodal MRI/CT molecular imaging [86].

In another research, L-cysteine coated FePt nanoparticles were developed for the dual CT/MR brain imaging and diagnosis of malignant gliomas. To this end, three different gliomas cells were used, and the CT images of the FePt-Cys nanoparticles indicated their higher enhancement compared to iohexol. The r2 of the nanoparticles was calculated to be 16.9 $mM^{-1}s^{-1}$ at 3.0 T magnetic field, which was lower compared to the FePt nanoparticles with Fe_2O_3 and SiO_2 coating. Use of cysteine as FePt nanoparticle coating has been associated with high biocompatibility, while Fe_2O_3 and SiO_2 coatings may be harmful to brain tissue [87]. Branca et al. reported the organometallic synthesis of FeBi nanoparticles with iron-enriched surfaces. The nanoparticles were synthesized with the sizes of 150 and 14 nanometers and coated with hydrophobic ligands. In addition, both the spherical nanoparticles contained distinct domains of Bi and Fe. The surface of the 150- and 14-nanometer particles was coated with amine ligands, and combination of an amine and its hydrochloride salt, respectively. Surface ligand treatment was also performed to provide water-soluble nanoparticles. It is notable that the functionalization of the nanoparticles with water-soluble ligands was only performed using larger FeBi particles due to the properties of their initial surface coating. The *in-vitro* results of T2-weighted MRI demonstrated that contrast enhancement increased at higher iron concentrations, suggesting that these nanoparticles could be applied as MRI contrast agent. Furthermore, the nanoparticles demonstrated higher X-ray attenuation compared to iodine-based CT contrast agents due to the higher X-ray absorption coefficient of bismuth. Therefore, the nanoprobe was introduced as an alternative to Fe/Au bimodal nanoprobes with the key advantage of cost-efficiency. The results of the mentioned study also emphasized on the importance of the initial surface coating of the nanoparticles in their further functionalization and transfer to water before their application in biomedical imaging [88].

CONCLUSION

Several bimodal imaging modalities are used for disease diagnosis since a single imaging modality cannot provide all the required data on various diseases. Bimodal MRI/CT has been developed to improve the accuracy and efficacy of disease diagnosis. Nanostructures are promising materials to be used as bimodal imaging probes. The present study aimed to review the current findings on bimodal MRI/CT nanoprobes and recent developments in this regard. To date, various nanostructures with different sizes, shapes, and coating materials have been investigated *in-vitro* and *in-vivo*, exhibiting the potential for application as bimodal MRI/CT nanoprobes. However, these nanoprobes have not been used clinically yet. Further investigations in this regard could be focused on the development of new

coating materials, such as inorganic materials and polymers.

ACKNOWLEDGMENTS

Hereby, we extend our gratitude to the Medical Radiation Sciences Research Group (MRSRG) at Tabriz University of Medical Sciences, Iran for the financial support of this research project (grant No. 58816).

REFERENCES

1. Miao X, Xu W, Cha H, Chang Y, Oh IT, Chae KS, Lee GH. Application of Dye-coated ultrasmall gadolinium oxide nanoparticles for biomedical dual imaging. Bull Korean Chem Soc. 2017; 38(9): 1058-1068.
2. Wei Z, Wu M, Li Z, Lin Z, Zeng J, Sun H, Liu X, Liu J, Li B, Zeng Y. Gadolinium-doped hollow CeO_2-ZrO_2 nanoplatform as multifunctional MRI/CT dual-modal imaging agent and drug delivery vehicle. Drug Deliv. 2018; 25(1): 353-363.
3. Hahn MA, Singh AK, Sharma P, Brown SC, Moudgil BM. Nanoparticles as contrast agents for in-vivo bioimaging: current status and future perspectives. Anal Bioanal Chem. 2011; 399(1): 3-27.
4. Li X, Zhang X-N, Li X-D, Chang J. Multimodality imaging in nanomedicine and nanotheranostics. Cancer biol med. 2016; 13(3): 339-348.
5. Padmanabhan P, Kumar A, Kumar S, Chaudhary RK, Gulyás B. Nanoparticles in practice for molecular-imaging applications: An overview. Acta biomater. 2016; 41:1-16.
6. Xia Y, Matham MV, Su H, Padmanabhan P, Gulyás B. Nanoparticulate contrast agents for multimodality molecular imaging. J Biomed Nanotechnol. 2016; 12(8):1553-1584.
7. Xing H, Bu W, Zhang S, Zheng X, Li M, Chen F, He Q, Zhou L, Peng W, Hua Y. Multifunctional nanoprobes for upconversion fluorescence, MR and CT trimodal imaging. Biomaterials. 2012; 33(4): 1079-1089.
8. Yang X, Hong H, Grailer JJ, Rowland IJ, Javadi A, Hurley SA, Xiao Y, Yang Y, Zhang Y, Nickles RJ. cRGD-functionalized, DOX-conjugated, and ^{64}Cu-labeled superparamagnetic iron oxide nanoparticles for targeted anticancer drug delivery and PET/MR imaging. Biomaterials. 2011; 32(17): 4151-4160.
9. Martí-Bonmatí L, Sopena R, Bartumeus P, Sopena P. Multimodality imaging techniques. Contrast Media Mol Imaging. 2010; 5(4): 180-189.
10. Cheheltani R, Ezzibdeh RM, Chhour P, Pulaparthi K, Kim J, Jurcova M, Hsu JC, Blundell C, Litt HI, Ferrari VA. Tunable, biodegradable gold nanoparticles as contrast agents for computed tomography and photoacoustic imaging. Biomaterials. 2016; 102: 87-97.
11. Nahas A, Varna M, Fort E, Boccara AC. Detection of plasmonic nanoparticles with full field-OCT: optical and photothermal detection. Biomed Opt Express. 2014; 5(10): 3541-3546.
12. Amendola V, Scaramuzza S, Litti L, Meneghetti M, Zuccolotto G, Rosato A, Nicolato E, Marzola P, Fracasso G, Anselmi C. Magneto-plasmonic Au-Fe alloy nanoparticles designed for multimodal SERS-MRI-CT imaging. Small. 2014; 10(12): 2476-2486.
13. Devaraj NK, Keliher EJ, Thurber GM, Nahrendorf M, Weissleder R. 18F labeled nanoparticles for in vivo PET-CT imaging. Bioconjug Chem. 2009; 20(2): 397-401.
14. Jin Y, Wang J, Ke H, Wang S, Dai Z. Graphene oxide modified PLA microcapsules containing gold nanoparticles for ultrasonic/CT bimodal imaging guided photothermal tumor therapy. Biomaterials. 2013; 34(20): 4794-4802.
15. An L, Hu H, Du J, Wei J, Wang L, Yang H, Wu D, Shi H, Li F, Yang S. Paramagnetic hollow silica nanospheres for in vivo targeted ultrasound and magnetic resonance imaging. Biomaterials. 2014; 35(20): 5381-5392.
16. Lee HY, Li Z, Chen K, Hsu AR, Xu C, Xie J, Sun S, Chen X. PET/MRI dual-modality tumor imaging using arginine-glycine-aspartic (RGD)–conjugated radiolabeled iron oxide nanoparticles. J Nucl Med. 2008; 49(8): 1371-1379.
17. Torres Martin de Rosales R, Tavaré R, Glaria A, Varma G, Protti A, Blower PJ. ^{99m}Tc-bisphosphonate-iron oxide nanoparticle conjugates for dual-modality biomedical imaging. Bioconjug Chem. 2011; 22(3): 455-465.
18. Eghbali P, Fattahi H, Laurent S, Muller RN, Oskoei YM. Fluorophore-tagged superparamagnetic iron oxide nanoparticles as bimodal contrast agents for MR/optical imaging. J Iran Chem Soc. 2016; 13(1): 87-93.
19. Sun M, Sundaresan G, Jose P, Yang L, Hoffman D, Lamichhane N, Zweit J. Highly stable intrinsically radiolabeled indium-111 quantum dots with multidentate zwitterionic surface coating: dual modality tool for biological imaging. J Mater Chem B. 2014; 2(28): 4456-4466.
20. Zheng X-Y, Sun L-D, Zheng T, Dong H, Li Y, Wang Y-F, Yan C-H. PAA-capped GdF_3 nanoplates as dual-mode MRI and CT contrast agents. Sci Bull. 2015; 60(12): 1092-1100.
21. Li X, Xiong Z, Xu X, Luo Y, Peng C, Shen M, Shi X. 99mTc-labeled multifunctional low-generation dendrimer-entrapped gold nanoparticles for targeted SPECT/CT dual-mode imaging of tumors. ACS Appl Mater Interfaces. 2016; 8(31): 19883-19891.
22. Zhang C, Zhou Z, Qian Q, Gao G, Li C, Feng L, Wang Q, Cui D. Glutathione-capped fluorescent gold nanoclusters for dual-modal fluorescence/X-ray computed tomography imaging. J Mater Chem B. 2013; 1(38): 5045-5053.
23. Key J, Leary JF. Nanoparticles for multimodal in vivo imaging in nanomedicine. Int J Nanomedicine. 2014; 9: 711-726.
24. Accardo A, Tesauro D, Aloj L, Pedone C, Morelli G. Supramolecular aggregates containing lipophilic Gd (III) complexes as contrast agents in MRI. Coord Chem Rev. 2009; 253(17-18): 2193-2213.
25. Boss A, Weiger M, Wiesinger F, editors. Future image acquisition trends for PET/MRI. Semin nucl med. 2015; 45(3): 201-211.
26. Wiesinger F, Sacolick LI, Menini A, Kaushik SS, Ahn S, Veit-Haibach P, Delso G, Shanbhag DD. Zero TE MR bone imaging in the head. Magn Reson Med. 2016; 75(1): 107-114.
27. Du F, Lou J, Jiang R, Fang Z, Zhao X, Niu Y, Zou S, Zhang M, Gong A, Wu C. Hyaluronic acid-functionalized bismuth oxide nanoparticles for computed tomography imaging-guided radiotherapy of tumor. Int J Nanomedicine. 2017; 12: 5973-5992.
28. Dekrafft KE, Xie Z, Cao G, Tran S, Ma L, Zhou OZ, Lin W. Iodinated nanoscale coordination polymers as potential

contrast agents for computed tomography. Angew Chem. 2009; 121(52): 10085-10088.
29. Kim D, Yu MK, Lee TS, Park JJ, Jeong YY, Jon S. Amphiphilic polymer-coated hybrid nanoparticles as CT/MRI dual contrast agents. Nanotechnology. 2011; 22(15): 155101.
30. Lee N, Choi SH, Hyeon T. Nano-sized CT contrast agents. Adv Mater. 2013; 25(19):2641-2660.
31. Liu Y, Ai K, Lu L. Nanoparticulate X-ray computed tomography contrast agents: from design validation to in vivo applications. Acc Chem Res. 2012; 45(10): 1817-1827.
32. Dadashi S, Poursalehi R, Delavari H. Optical and structural properties of oxidation resistant colloidal bismuth/gold nanocomposite: an efficient nanoparticles based contrast agent for X-ray computed tomography. J Mol Liq. 2018; 254: 12-19.
33. Hernández-Rivera M, Kumar I, Cho SY, Cheong BY, Pulikkathara MX, Moghaddam SE, Whitmire KH, Wilson LJ. High-performance hybrid bismuth–carbon nanotube based contrast agent for X-ray CT imaging. ACS Appl Mater Interfaces. 2017; 9(7): 5709-5716.
34. Chen J, Yang X-Q, Meng Y-Z, Huang H-H, Qin M-Y, Yan D-M, Zhao Y-D, Ma Z-Y. In vitro and in vivo CT imaging using bismuth sulfide modified with a highly biocompatible Pluronic F127. Nanotechnology. 2014; 25(29): 295103.
35. Li Z, Hu Y, Howard KA, Jiang T, Fan X, Miao Z, Sun Y, Besenbacher F, Yu M. Multifunctional bismuth selenide nanocomposites for antitumor thermo-chemotherapy and imaging. ACS nano. 2016; 10(1): 984-997.
36. Aydogan B, Li J, Rajh T, Chaudhary A, Chmura SJ, Pelizzari C, Wietholt C, Kurtoglu M, Redmond P. AuNP-DG: deoxyglucose-labeled gold nanoparticles as X-ray computed tomography contrast agents for cancer imaging. Mol Imaging Biol. 2010; 12(5): 463-467.
37. Shaabani E, Amini SM, Kharrazi S, Tajerian R. Curcumin coated gold nanoparticles: synthesis, characterization, cytotoxicity, antioxidant activity and its comparison with citrate coated gold nanoparticles. Nanomed J. 2017; 4(2):115-125.
38. Verissimo TV, Santos NT, Silva JR, Azevedo RB, Gomes AJ, Lunardi CN. In vitro cytotoxicity and phototoxicity of surface-modified gold nanoparticles associated with neutral red as a potential drug delivery system in phototherapy. Mater Sci Eng C. 2016; 65: 199-204.
39. Kubíčková L. Relaxivity of magnetic iron oxide nanoparticles containing diamagnetic cations. 2017.
40. Ta HT, Li Z, Wu Y, Cowin G, Zhang S, Yago A, Whittaker AK, Xu ZP. Effects of magnetic field strength and particle aggregation on relaxivity of ultra-small dual contrast iron oxide nanoparticles. Mater Res Express. 2017; 4(11): 116105.
41. Park JY, Baek MJ, Choi ES, Woo S, Kim JH, Kim TJ, Jung JC, Chae KS, Chang Y, Lee GH. Paramagnetic ultrasmall gadolinium oxide nanoparticles as advanced T1 MRI contrast agent: account for large longitudinal relaxivity, optimal particle diameter, and in vivo T1 MR images. ACS Nano. 2009; 3(11): 3663-3669.
42. Roohi F, Lohrke J, Ide A, Schütz G, Dassler K. Studying the effect of particle size and coating type on the blood kinetics of superparamagnetic iron oxide nanoparticles. Int J Nanomedicine. 2012; 7: 4447-4458.
43. Park JY, Kim SJ, Lee GH, Jin S, Chang Y, Bae JE, Chae KS. Various ligand-coated ultrasmall gadolinium-oxide nanoparticles: Water proton relaxivity and in-vivo T1 MR image. J Korean Phys Soc. 2015; 66(8): 1295-1302.
44. Estelrich J, Sánchez-Martín MJ, Busquets MA. Nanoparticles in magnetic resonance imaging: from simple to dual contrast agents. Int J Nanomedicine. 2015; 10: 1727-1741.
45. Lusic H, Grinstaff MW. X-ray-computed tomography contrast agents. Chem Rev. 2013; 113(3): 1641-1666.
46. Yin J, Chen D, Zhang Y, Li C, Liu L, Shao Y. MRI relaxivity enhancement of gadolinium oxide nanoshells with a controllable shell thickness. Phys Chem Chem Phys. 2018; 20(15): 10038-10047.
47. Luo N, Tian X, Xiao J, Hu W, Yang C, Li L, Chen D. High longitudinal relaxivity of ultra-small gadolinium oxide prepared by microsecond laser ablation in diethylene glycol. J Appl Phys. 2013; 113(16): 164306.
48. Faucher L, Gossuin Y, Hocq A, Fortin M-A. Impact of agglomeration on the relaxometric properties of paramagnetic ultra-small gadolinium oxide nanoparticles. Nanotechnology. 2011; 22(29): 295103(10pp).
49. Fang J, Chandrasekharan P, Liu X-L, Yang Y, Lv Y-B, Yang C-T, Ding J. Manipulating the surface coating of ultra-small Gd_2O_3 nanoparticles for improved T1-weighted MR imaging. Biomaterials. 2014; 35(5): 1636-1642.
50. Engström M, Klasson A, Pedersen H, Vahlberg C, Käll P-O, Uvdal K. High proton relaxivity for gadolinium oxide nanoparticles. Magn Reson Mater Phy. 2006; 19(4): 180-186.
51. Babić-Stojić B, Jokanović V, Milivojević D, Požek M, Jagličić Z, Makovec D, Arsikin K, Paunović V. Gd_2O_3 nanoparticles stabilized by hydrothermally modified dextrose for positive contrast magnetic resonance imaging. J Magn Magn Mater. 2016; 403: 118-126.
52. Ahmad MW, Xu W, Kim SJ, Baeck JS, Chang Y, Bae JE, Chae KS, Park JA, Kim TJ, Lee GH. Potential dual imaging nanoparticle: Gd_2O_3 nanoparticle. Sci Rep. 2015; 5: 8549.
53. Carrascosa P, Capuñay C, Deviggiano A, Bettinotti M, Goldsmit A, Tajer C, Carrascosa J, García MJ. Feasibility of 64-slice gadolinium-enhanced cardiac CT for the evaluation of obstructive coronary artery disease. Heart. 2010; 96(19): 1543-1549.
54. Regino CAS, Walbridge S, Bernardo M, Wong KJ, Johnson D, Lonser R, Oldfield EH, Choyke PL, Brechbiel MW. A dual CT-MR dendrimer contrast agent as a surrogate marker for convection-enhanced delivery of intracerebral macromolecular therapeutic agents. Contrast Media Mol Imaging. 2008; 3(1): 2-8.
55. Kim D, Park S, Lee JH, Jeong YY, Jon S. Antibiofouling polymer-coated gold nanoparticles as a contrast agent for in vivo X-ray computed tomography imaging. J Am Chem Soc. 2007; 129(24): 7661-7665.
56. Tian C, Zhu L, Lin F, Boyes SG. Poly (acrylic acid) bridged gadolinium metal–organic framework–gold nanoparticle composites as contrast agents for computed tomography and magnetic resonance bimodal imaging. ACS Appl Mater Interfaces. 2015; 7(32): 17765-17775.
57. Sun H, Yuan Q, Zhang B, Ai K, Zhang P, Lu L. GdIII functionalized gold nanorods for multimodal imaging applications. Nanoscale. 2011; 3(5): 1990-1996.
58. Alric C, Taleb J, Le Duc G, Mandon C, Billotey C, Le Meur-Herland A, Brochard T, Vocanson F, Janier M, Perriat P, Roux S, Tillement O. Gadolinium chelate coated gold nanoparticles as contrast agents for both X-ray computed tomography and magnetic resonance imaging. J Am Chem Soc. 2008; 130(18): 5908-5915.
59. Zhou B, Xiong Z, Zhu J, Shen M, Tang G, Peng C, Shi X.

PEGylated polyethylenimine-entrapped gold nanoparticles loaded with gadolinium for dual-mode CT/MR imaging applications. Nanomedicine. 2016; 11(13): 1639-1652.
60. Zhao W, Chen L, Wang Z, Huang Y, Jia N. An albumin-based gold nanocomposites as potential dual mode CT/MRI contrast agent. J Nanopart Res. 2018; 20(2): 40.
61. Li K, Wen S, Larson AC, Shen M, Zhang Z, Chen Q, Shi X, Zhang G. Multifunctional dendrimer-based nanoparticles for in vivo MR/CT dual-modal molecular imaging of breast cancer. Int J Nanomedicine. 2013; 8: 2589-2600.
62. Chen Q, Wang H, Liu H, Wen S, Peng C, Shen M, Zhang G, Shi X. Multifunctional dendrimer-entrapped gold nanoparticles modified with RGD peptide for targeted computed tomography/magnetic resonance dual-modal imaging of tumors. Anal Chem. 2015; 87(7): 3949-3956.
63. Li X, Wu M, Wang J, Dou Y, Gong X, Liu Y, Guo Q, Zhang X, Chang J, Niu Y. Ultrasmall bimodal nanomolecules enhanced tumor angiogenesis contrast with endothelial cell targeting and molecular pharmacokinetics. Nanomedicine: NBM. 2019; 15:252-263.
64. Yu S-B, Watson AD. Metal-based X-ray contrast media. Chem Rev. 1999; 99(9): 2353-2378.
65. Rameshbabu N, Sampath Kumar TS, Prabhakar TG, Sastry VS, Murty KVGK, Prasad Rao K. Antibacterial nanosized silver substituted hydroxyapatite: Synthesis and characterization. J Biomed Mater Res A. 2007; 80A(3): 581-591.
66. Madhumathi K, Kumar S, Sanjeed M, Muhammed S, Nazrudeen S. Silver and gadolinium ions co-substituted hydroxyapatite nanoparticles as bimodal contrast agent for medical imaging. Bioceram Dev Appl. 2014; 4: 1-4.
67. Jin X, Fang F, Liu J, Jiang C, Han X, Song Z, Chen J, Sun G, Lei H, Lu L. An ultrasmall and metabolizable PEGylated NaGdF 4: Dy nanoprobe for high-performance T 1/T 2-weighted MR and CT multimodal imaging. Nanoscale. 2015; 7(38): 15680-15688.
68. Wang T, Jia G, Cheng C, Wang Q, Li X, Liu Y, He C, Chen L, Sun G, Zuo C. Active targeted dual-modal CT/MR imaging of VX2 tumors using PEGylated $BaGdF_5$ nanoparticles conjugated with RGD. New J Chem. 2018; 42(14): 11565-11572.
69. Li L, Lu Y, Lin Z, Mao AS, Jiao J, Zhu Y, Jiang C, Yang Z, Peng M, Mao C. Ultralong tumor retention of theranostic nanoparticles with short peptide-enabled active tumor homing. Mater Horiz. 2019 (In press), DOI: 10.1039/c9mh00014c.
70. Pan D, Schmieder AH, Wickline SA, Lanza GM. Manganese-based MRI contrast agents: past, present and future. Tetrahedron. 2011; 67(44): 8431-8444.
71. Wang R, Luo Y, Yang S, Lin J, Gao D, Zhao Y, Liu J, Shi X, Wang X. Hyaluronic acid-modified manganese-chelated dendrimer-entrapped gold nanoparticles for the targeted CT/MR dual-mode imaging of hepatocellular carcinoma. Sci Rep. 2016; 6: 33844.
72. Simao T, Chevallier P, Lagueux J, Côté M-F, Rehbock C, Barcikowski S, Fortin M-A, Guay D. Laser-synthesized ligand-free Au nanoparticles for contrast agent applications in computed tomography and magnetic resonance imaging. J Mater Chem B. 2016; 4(39): 6413-6427.
73. Gharehaghaji N, Divband B. A novel MRI contrast agent synthesized by ion exchange method. Nanomed J. 2018; 5(1): 15-18.
74. Amoli-Diva M, Daghighi Asli M, Karimi S. FeMn2O4 nanoparticles coated dual responsive temperature and pH-responsive polymer as a magnetic nano-carrier for controlled delivery of letrozole anti-cancer. Nanomed J. 2017; 4(4): 218-223.
75. Kim DK KJ, Jeong YY, Jon SY. Antibiofouling polymer coated gold@iron oxide nanoparticle (GION) as a dual contrast agent for CT and MRI. Bull Korean Chem Soc. 2009; 30(8): 1855-1857.
76. Narayanan S, Sathy BN, Mony U, Koyakutty M, Nair SV, Menon D. Biocompatible magnetite/gold nanohybrid contrast agents via green chemistry for MRI and CT bioimaging. ACS Appl Mater Interfaces. 2012; 4(1): 251-260.
77. Cai H, Li K, Shen M, Wen S, Luo Y, Peng C, Zhang G, Shi X. Facile assembly of Fe3O4@Au nanocomposite particles for dual mode magnetic resonance and computed tomography imaging applications. J Mater Chem. 2012; 22(30): 15110-15120.
78. Li J, Zheng L, Cai H, Sun W, Shen M, Zhang G, Shi X. Facile one-pot synthesis of Fe_3O_4@Au composite nanoparticles for dual-mode MR/CT imaging applications. ACS Appl Mater interfaces. 2013; 5(20): 10357-10366.
79. Zhu J, Lu Y, Li Y, Jiang J, Cheng L, Liu Z, Guo L, Pan Y, Gu H. Synthesis of Au–Fe3O4 heterostructured nanoparticles for in vivo computed tomography and magnetic resonance dual model imaging. Nanoscale. 2014; 6(1): 199-202.
80. Wang G, Gao W, Zhang X, Mei X. Au Nanocage functionalized with ultra-small Fe_3O_4 nanoparticles for targeting T1–T2 dual MRI and CT imaging of tumor. Sci Rep. 2016; 6: 28258.
81. Lee N, Cho HR, Oh MH, Lee SH, Kim K, Kim BH, Shin K, Ahn T-Y, Choi JW, Kim Y-W. Multifunctional Fe_3O_4/TaOx core/shell nanoparticles for simultaneous magnetic resonance imaging and X-ray computed tomography. J Am Chem Soc. 2012; 134(25): 10309-10312.
82. Zhu J, Wang J, Wang X, Zhu J, Yang Y, Tian J, Cui W, Ge C, Li Y, Pan Y, Gu H. Facile synthesis of magnetic core–shell nanocomposites for MRI and CT bimodal imaging. J Mater Chem B. 2015; 3 (34): 6905-6910.
83. Badrigilan S, Shaabani B, Gharehaghaji N, Mesbahi A. Iron oxide/bismuth oxide nanocomposites coated by graphene quantum dots:"Three-in-one" theranostic agents for simultaneous CT/MR imaging-guided in vitro photothermal therapy. Photodiagnosis Photodyn Ther. 2019; 25: 504-514.
84. Gharehaghaji N, Divband B, Zareei L. Nanoparticulate NaA zeolite composites for MRI: Effect of iron oxide content on image contrast. J Magn Magn Mater. 2018; 456: 136-141.
85. Atashi Z, Divband B, Keshtkar A, Khatamian M, Farahmand-Zahed F, Nazarlo AK, Gharehaghaji N. Synthesis of cytocompatible Fe_3O_4@ ZSM-5 nanocomposite as magnetic resonance imaging contrast agent. J Magn Magn Mater. 2017; 438: 46-51.
86. Chou S-W, Shau Y-H, Wu P-C, Yang Y-S, Shieh D-B, Chen C-C. In vitro and in vivo studies of FePt nanoparticles for dual modal CT/MRI molecular imaging. J Am Chem Soc. 2010; 132(38): 13270-13278.
87. Liang S, Zhou Q, Wang M, Zhu Y, Wu Q, Yang X. Water-soluble L-cysteine-coated FePt nanoparticles as dual MRI/CT imaging contrast agent for glioma. Int J Nanomedicine. 2015; 10: 2325-2333.
88. Branca M, Pelletier F, Cottin B, Ciuculescu D, Lin CC, Serra R, Mattei JG, Casanove MJ, Tan R, Respaud M, Amiens C. Design of FeBi nanoparticles for imaging applications. Faraday Discuss. 2014; 175: 97-111.